Journal of Oceanography (2018) 74:305–317
https://doi.org/10.1007/s10872-017-0460-y

ORIGINAL ARTICLE

Spatial distribution of dissolved methane and its source in the western Arctic Ocean

Kushi Kudo[1] · Keita Yamada[2] · Sakae Toyoda[2] · Naohiro Yoshida[1,2,3] · Daisuke Sasano[4] · Naohiro Kosugi[5] · Masao Ishii[5] · Hisayuki Yoshikawa[6] · Akihiko Murata[7] · Hiroshi Uchida[7] · Shigeto Nishino[7]

Received: 2 August 2017 / Revised: 24 December 2017 / Accepted: 27 December 2017 / Published online: 12 January 2018
© The Oceanographic Society of Japan and Springer Japan KK, part of Springer Nature 2018

Abstract

Recent Arctic warming and decreasing sea-ice can promote the release of methane (CH_4), a greenhouse gas, from the Arctic Ocean, thereby providing a strong climate feedback. However, the dynamics of dissolved CH_4 in the Arctic Ocean remain uncertain, especially in western areas. This report describes the horizontal and vertical distributions of concentration and stable carbon isotope ratio ($\delta^{13}C$ value) of CH_4 in the western Arctic Ocean. Surface layer samples used for this study were supersaturated with CH_4 in comparison to the atmosphere. Especially high CH_4 concentrations (up to 10.3 nmol kg^{-1}) were observed at stations in the continental shelf area. At the bottom layer of the shelf stations, the CH_4 concentration was higher (up to 55.9 nmol kg^{-1}). Its $\delta^{13}C$ value was lower (down to − 63.8‰) than in the surface layer, which suggests that CH_4 in the shelf water is produced mainly by methanogens in sediment. At deeper stations in the Canada Basin (seafloor > 300 m depth), the maxima of CH_4 concentration were detected at depths of 10–50 m and 100–200 m, although $\delta^{13}C$ values were lowest at 50 m depth. The shallower CH_4 maximum coincided with the DO maximum, suggesting CH_4 production by plankton activity or sinking particles. The deeper CH_4 maximum corresponded to the nutrient maximum, suggesting horizontal advection of shelf water from the coastal shelf area. From the results, we were able to confirm that the dynamics of dissolved CH_4 in the western Arctic Ocean in summer 2012 varied with area and depth.

Keywords Western Arctic Ocean · Dissolved CH_4 concentration · Stable carbon isotope ratio · Depth profile · Chukchi Sea · Canada Basin · Bering Strait · Organic matter degradation from sediment · Methanogen · Plankton activity

1 Introduction

Because of recent global warming, a sea-ice decrease can be measured in the Arctic Ocean especially during summer (McGuire et al. 2009, 2010; Arrigo and van Dijken 2011; Permenteir et al. 2013). During 1979–2012, the respective rates of decrease of the annual mean Arctic sea-ice extent

Electronic supplementary material The online version of this article (https://doi.org/10.1007/s10872-017-0460-y) contains supplementary material, which is available to authorized users.

✉ Kushi Kudo
kudo.k.ab@m.titech.ac.jp

[1] Department of Environmental Chemistry and Engineering, Tokyo Institute of Technology, 4259 Nagatsuta, Midori-ku, Yokohama 226-8502, Japan

[2] Department of Chemical Science and Engineering, Tokyo Institute of Technology, 4259 Nagatsuta, Midori-ku, Yokohama 226-8502, Japan

[3] Earth-life Science Institute, Tokyo Institute of Technology, 2-12-1-IE-1 Ookayama, Meguro-ku, Tokyo 125-8550, Japan

[4] Japan Meteorological Agency, 1-3-4 Otemachi, Chiyoda-ku, Tokyo 100-8122, Japan

[5] Meteorological Research Institute (MRI), 1-1 Nagamine, Tsukuba 305-0052, Japan

[6] Faculty of Environmental Earth Science, Hokkaido University, N10 W5, Kita-ku, Sapporo 060-0810, Japan

[7] Japan Agency for Marine-Earth Science and Technology (JAMSTEC), 2-15 Natsushimamachi, Yokosuka 237-0061, Japan

and the summer sea-ice minimum have been 3.5–4.1% per decade and 9.4–13.6% per decade (IPCC 2013). These sea-ice decreases affect heat, light, and freshwater cycles in this area, accelerating primary production and seafloor sediments (McGuire et al. 2009, 2010; Arrigo and van Dijken 2011; Hioki et al. 2014; Harada 2016). These phenomena might accelerate the release of greenhouse gases. In particular, the release of methane (CH_4) has been regarded as predominant because of its greater storage capacity in Arctic areas (35–365 Pg CH_4) (IPCC 2007, 2013; McGuire et al. 2009, 2010; Dlugokencky et al. 2009, 2011).

Terrestrial and oceanic CH_4 in Arctic areas are potentially important sources to the atmosphere. Their flux is estimated at 32–112 Tg C $year^{-1}$ (McGuire et al. 2009, 2010). In the Arctic Ocean, CH_4 production has been reported via processes of CH_4 release from seafloor sediments in the Beaufort Sea, Eastern Siberian Sea, Laptev Sea, and off the Svalbard islands (Kvenvolden et al. 1993; Damm et al. 2005, 2008; Shakhova et al. 2005, 2010, 2014; Myhre et al. 2016), in addition to aerobic CH_4 production by the phytoplankton metabolite dimethylsulfoniopropionate (DMSP: $(CH_3)_2S^+CH_2CH_2COO^-$) in the central Arctic Ocean (Damm et al. 2010). These CH_4 production processes and dynamics of dissolved CH_4 affect the budget, influencing not only the Arctic climate but also global climate (e.g., IPCC 2013).

Earlier studies revealed the characteristic stable carbon isotope ratio ($\delta^{13}C$, see Sect. 2.2 for definition) of oceanic CH_4 produced by various processes. (1) Biogenic sources such as sedimentary organic matter and CH_4 clathrate hydrate are divided into two pathways: (a) CO_2 reduction pathway ($CO_2 + 4H_2 \rightarrow CH_4 + 2H_2O$, mainly occurring in seawater) and (b) acetate fermentation pathway ($CH_3COOH \rightarrow CH_4 + CO_2$, mainly occurring in freshwater). In seawater, acetate is used as a substance of such sulfate-reducing bacteria. Therefore, CH_4 formation occurs almost entirely via the CO_2 reduction pathway in seawater (e.g., Whiticar 1999). The $\delta^{13}C$ values of CH_4 produced by CO_2 reduction were reported as − 110 to − 60‰ (Whiticar et al. 1986; Whiticar 1999; Kvenvolden 1993; Kastner et al. 1998). The reported $\delta^{13}C$ values of CH_4 produced by acetate fermentation are − 65 to − 50‰ (Whiticar et al. 1986; Whiticar 1999). (2) Thermogenic processes in hydrothermal systems produce CH_4 with $\delta^{13}C$ values of − 50 to − 20‰ (Whiticar et al. 1986; Whiticar 1999). (3) In aerobic environments, methanogenic archaea living within anaerobic cavities of the zooplankton gut or inside sinking particles produce CH_4. Their respective reported $\delta^{13}C$ values are − 61 to − 54‰ (Sasakawa et al. 2008) and − 37 to + 6‰ (Sasakawa et al. 2008). Oceanic CH_4 is consumed mainly by microbial CH_4 oxidation, and then the $\delta^{13}C$ value becomes higher (e.g., Sansone et al. 2001; Yoshikawa et al. 2014). In the Arctic Ocean, reports of several studies have described the concentration and $\delta^{13}C$ of CH_4. Macdonald (1976) observed vertical profile of CH_4 concentration in 1974 and 1975 in the Beaufort Sea. That study found concentrations near equilibrium with the atmosphere (approx. 3.5 nmol L^{-1}) in surface waters but concentrations considerably higher than saturation near the bottom layer (up to 50 nmol L^{-1}) during the sea-ice melted season. Shakhova et al. (2005) measured CH_4 concentration in the East Siberian and Laptev Seas in the summers of 2003 and 2004. They found that CH_4 concentrations in the surface layer were 2.1–28.2 nmol L^{-1} in 2003 and approx. 5–110 nmol L^{-1} in plume areas in 2004. In the bottom layer, it was approx. 5–87 nmol L^{-1} in 2003 and approx. 5–154 nmol L^{-1} in 2004. Kvenvolden et al. (1993) observed that microbubbles in sea ice in the Beaufort Sea have a high concentration of CH_4, with $\delta^{13}C$ of − 78.4‰. Damm et al. (2005, 2008, 2010, 2015) reported that sources of CH_4 in Pacific-derived water (Pdw) ($\delta^{13}C < -46$‰) and Atlantic-derived water (Adw) ($\delta^{13}C = -43$ to − 41‰) in the central Arctic Ocean differ. They inferred a CH_4 surplus in Pdw and mixing between the local marine background (− 38‰) and the atmospheric reservoir (− 47‰) in Adw. Savvichev et al. (2007) observed CH_4 profiles in the water column and bottom sediments of the Bering Strait and Chukchi Sea. They found that the CH_4 content in the water column of the Chukchi Sea varied from 8 to 31 nmol L^{-1}, and that the CH_4 formation rate from bottom sediments varied from 0.25 to 16 nmol dm^{-3} day^{-1}. Fenwick et al. (2017) observed dissolved CH_4 with its concentration of 0.7–30.5 nmol L^{-1} ($\delta^{13}C = -42$ to − 33‰) in the Bering Sea and Chukchi Sea in summer 2015. They concluded that dissolved CH_4 was produced mainly from seafloor sediments via the decomposition of organic carbon. Then microbial CH_4 oxidation occurred. Lapham et al. (2017) reported that CH_4 concentrations in Barrow Canyon were 5–74 nmol L^{-1} in August 2012. They inferred that CH_4 was produced mainly from sedimentary sources.

Nevertheless, data of CH_4 obtained in the western Arctic Ocean (Bering Sea, Chukchi Sea and Canada Basin) are almost nonexistent. Few studies have used $\delta^{13}C$ of CH_4, which provides information about CH_4 production and consumption processes, including its concentration (e.g., Kvenvolden et al. 1993). Therefore, identification of the influence on CH_4 amounts, its production and consumption processes, and its cycle (e.g., McGuire et al. 2009) in the Arctic Ocean remains difficult.

Therefore, the present study surveys and analyzes the distribution of CH_4 dissolved in the surface water and the water column of the western Arctic Ocean. We investigated CH_4 production and consumption processes by first elucidating the CH_4 concentration and $\delta^{13}C$.

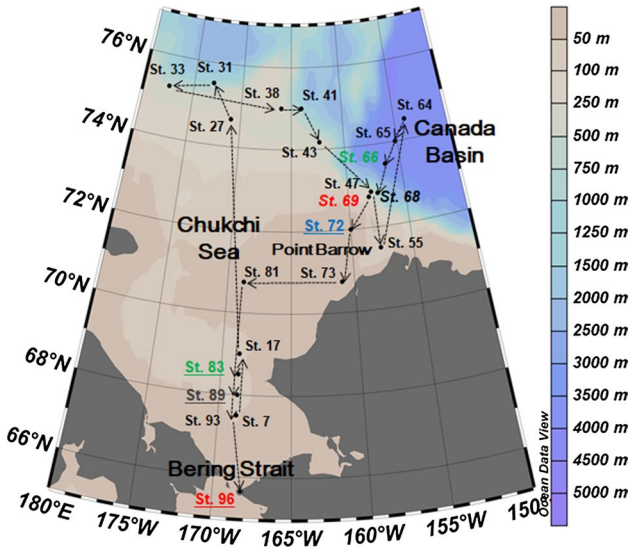

Fig. 1 Map of sampling stations. Broken arrows represent the cruise track of R/V Mirai. Stations which have vertical profiles are underlined and colored as in the coastal shelf area and in italics in the deeper area (color figure online)

2 Instruments and methods

2.1 Sampling

During the MR12-E03 cruise of R/V Mirai (JAMSTEC, Japan), as a part of the GRENE Arctic Climate Change Research Project (Fig. 1), we collected seawater samples at 26 stations (St.) in the western Arctic Ocean from 15 September to 4 October in 2012. During the sampling period, sea ice was almost free around the sampling stations. Of those stations, 15 were located at continental shelf areas (Bering Sea, Chukchi Sea, part of the Chukchi Plateau, and off Point Barrow; seafloor ≤ 300 m depth); 11 were in deeper areas (part of the Chukchi Plateau and edge of Canada Basin; seafloor > 300 m depth). Samples were collected using a CTD-CAROUSEL system (Sea-Bird Electronics, Bellevue, WA, USA) equipped with 12-L Niskin bottles at two or three depths at the continental shelf stations and 5–20 depths at the deeper stations. Samples were subsampled, respectively, into 30-mL and 125-mL glass vials for analyses of their concentrations and stable carbon isotope ratios of CH_4. Special care was taken to avoid air contamination. These samples were sterilized by adding saturated mercuric chloride ($HgCl_2$) solution (final $HgCl_2$ concentration was ca. 0.5%; Karl and Tilbrook 1994; Watanabe et al. 1995) and were sealed with rubber stoppers and aluminum caps. They were stored in a refrigerator (dark, 277 K) until analysis. Measurements of water temperature, salinity, dissolved oxygen, nutrients, total inorganic carbon, and total alkalinity were conducted onboard (Kikuchi 2012, R/V Mirai Cruise Report MR12-E03, edited by T. Kikuchi and S. Nishino 190 pp., JAMSTEC, Yokosuka, Japan).

2.2 Concentration and isotopic measurement of dissolved CH_4

The concentration and stable carbon isotope ratio of dissolved CH_4 were measured, respectively, using gas chromatography with flame ionization detection (GC-FID) and gas chromatography combustion isotope ratio mass spectrometry (GC-C-IRMS). For each measurement, the dissolved CH_4 was extracted with a purge and trap unit. We extracted the dissolved CH_4 using a glass gas extraction bottle (125 mL) and a trap cooled with liquid N_2 (170-mm-long column packed with Polapak-Q and glass wool) based on a description by Tsunogai et al. (1998, 2000). Then the dissolved CH_4 was injected into the GC by He carrier gas. For isotopic measurements, CH_4 was separated from interfering components (CO) using a column packed with molecular sieves 5A (10 mm ID × 500 mm length, 30/60 mesh, GL Sciences, Inc., Tokyo, Japan) before it was concentrated in a cryofocusing trap. The $\delta^{13}C$ value was calculated as shown below:

$$\delta^{13}C = (({}^{13}C/{}^{12}C)_{sample}/({}^{13}C/{}^{12}C)_{VPDB^{-1}}) \times 1000. \quad (1)$$

Therein, VPDB stands for Vienna Pee Dee Belemnite, the international standard of the $^{13}C/^{12}C$ ratio.

We used two working standards. For concentration measurements, we used 2.08 ppm CH_4 in purified air (Taiyo Nissan Co.). For isotope measurements, 1000 ppm CH_4 in He (Taiyo Nissan Co.) with $\delta^{13}C = -39.56‰$ was used (Yamada et al. 2005). Precision of the concentration and $\delta^{13}C$ value of CH_4 were estimated respectively as < 5% ($n = 5$, 1σ) and < 0.3‰ ($n = 6$, 1σ) based on repeated analyses of the standards. The differences between measured concentrations and $\delta^{13}C$ of duplicate seawater samples were, respectively, 0.1–0.7 nmol kg^{-1} and 0.1–0.8‰.

2.3 Data analysis

We calculated the oversaturation ratio (SR) of dissolved CH_4 using its solubility (Wiesenberg and Guinasso 1979) of

$$SR(\%) = ([[CH_4]_w/[CH_4]_a] - 1) \times 100, \quad (2)$$

where $[CH_4]_w$ denotes the measured concentration and $[CH_4]_a$ represents the equilibrium concentration calculated from the atmospheric concentration of CH_4 ($f_G = 1.89$ ppmv: Database of JAMSTEC), seawater temperature (T, in K), and salinity (S, ‰) as

$$\ln[CH_4]_a = \ln f_G + A_1 + A_2(100/T) + A_3 \ln(T/100) + A_4(T/100) + S[B_1 + B_2(T/100) + B_3(T/100)^2], \quad (3)$$

where $A_1 = -417.5023$, $A_2 = 599.8626$, $A_3 = 380.3636$, $A_4 = -62.0764$, $B_1 = -0.064236$, $B_2 = 0.034980$, and $B_3 = -0.0052732$.

Sea–air CH_4 flux (F_{CH4}, μmol m^{-2} day^{-1}) was calculated according to a description by Wanninkhof (1992):

$$F_{CH_4} = k_w \times ([CH_4]_{w(0-10m)} - [CH_4]_a). \quad (4)$$

Therein $[CH_4]_{w(0-10m)}$ stands for the measured CH_4 concentration in the surface 0–10 m seawater. Also k_w denotes the gas transfer velocity, which depends on the wind speed (v, m s^{-1}) at 10 m overseas height and which is calculated using the equation below:

$$k_w = 0.31v^2\sqrt{(Sc/660)^{-1}}. \quad (5)$$

In that equation, Sc represents the Schmidt number of CH_4 in seawater, which depends on the atmospheric temperature (T, in °C) and which is calculated as presented below:

$$Sc = 2039.2 - 120.31T + 3.4029T^2 - 0.040437T^3. \quad (6)$$

The atmospheric temperature and wind speeds in Eqs. (5) and (6) were taken from the integrated meteorological dataset obtained during the MR12-E03 cruise [Japan Agency for Marine-Earth Science and Technology (2016) Data Research System for Whole Cruise Information in JAMSTEC. http://www.godac.jamstec.go.jp/darwin/].

Assuming that CH_4 dissolved in excess (SR > 0) is a mixture of atmospheric CH_4 and CH_4 produced in the water column, we calculated the $\delta^{13}C$ value of the excess CH_4 ($\delta^{13}C_{ex}$) based on the mass balance as shown below (Sasakawa et al. 2008):

$$\delta^{13}C_{ex} = (\delta^{13}C \times [CH_4] - \delta^{13}C_a \times [CH_4]_a)/[CH_4]_{ex}. \quad (7)$$

In that equation, $\delta^{13}C_a$ represents the $\delta^{13}C$ value of the atmospheric equilibrium (= − 47‰ VPDB: Quay et al. 1991; Grant and Whiticar 2002)

We also examined the possibility of microbial oxidation of CH_4 in the water column using the following equation (Coleman et al. 1981):

$$\delta^{13}C = \delta^{13}C_{t_0} + 1000 \times (1/\alpha - 1) \times \ln([CH_4]/[CH_4]_{t_0}). \quad (8)$$

In that equation, t_0 stands for the initial state before oxidation of CH_4. Also, α denotes the kinetic isotope fractionation factor, which was obtained from incubation experiments. Equation (8) is applicable if we assume that the CH_4 concentration is controlled simply by microbial oxidation in a closed system.

3 Results

3.1 Dissolved CH_4 dynamics in surface seawater

The respective distributions of concentration, oversaturation ratio (SR), sea–air CH_4 flux (F_{CH4}), and $\delta^{13}C$ values of dissolved CH_4 in seawater are presented in Fig. 2a–d. Information related to wind speed, air temperature, dissolved and atmospheric equilibrium CH_4 concentration, sea–air CH_4 flux, and values of $\delta^{13}C$ and $\delta^{13}C_{ex}$ of dissolved CH_4 in the surface water and atmospheric CH_4 is shown in Table S1.

Surface water was found to be supersaturated with CH_4 at all stations (SR = 5.1–206.2%, Fig. 2b, Table S1). In general, CH_4 concentrations were higher at the stations at continental shelf areas (5.5 ± 0.4 nmol kg^{-1}, average and 1σ) than at the stations at deeper areas (4.7 ± 0.1 nmol kg^{-1}). Especially high CH_4 concentrations were observed off Point Barrow (up to 10.3 nmol kg^{-1}).

The $\delta^{13}C$ values of dissolved CH_4 were − 55.0 to − 41.1‰ (average and 1σ, − 47.1 ± 1.3‰) (Table S1, Fig. 2c). The $\delta^{13}C$ values at continental shelf areas (average, $\delta^{13}C$ = − 48.9 ± 2.2‰) were lower than the values of atmospheric equilibrium CH_4 (− 47‰), although the $\delta^{13}C$ values in deeper areas (− 45.3 ± 1.3‰) were often higher than the values of atmospheric equilibrium CH_4. Especially low $\delta^{13}C$ values (down to − 55.9‰) were observed off Point Barrow. Calculated $\delta^{13}C_{ex}$ values were − 67.2 to − 14.8‰.

3.2 Vertical distribution of dissolved CH_4

3.2.1 Continental shelf area

Figure 3a–f and Table S2 present vertical distributions of dissolved CH_4, dissolved oxygen (DO), and physical parameters of seawater in the continental shelf area (St. 72, 83, 89, and 96). In the Chukchi Sea (St. 72, 83, and 89), CH_4 concentrations increased with depth [surface, $[CH_4]$ = 4.1–6.1 nmol kg^{-1}, SR = 14.0–65.5%; bottom, $[CH_4]$ = 16.9–55.9 nmol kg^{-1}, SR = 398.1–1386.8% (Fig. 3a, b)], whereas $\delta^{13}C$–CH_4 values decreased with depth (surface, − 55.0 to − 49.4‰; bottom, − 63.8 to − 61.3‰) (Fig. 3c). However, in the Bering Strait in October (St. 96), the vertical gradient of concentration and $\delta^{13}C$ value was small, showing an almost homogeneous vertical distribution (surface, $[CH_4]$ = 5.1 nmol kg^{-1}, SR = 48.0%, $\delta^{13}C$–CH_4 = − 48.2‰; bottom, $[CH_4]$ = 6.3 nmol kg^{-1}, SR = 80.2%, $\delta^{13}C$–CH_4 = − 47.4‰) (Fig. 3a–c).

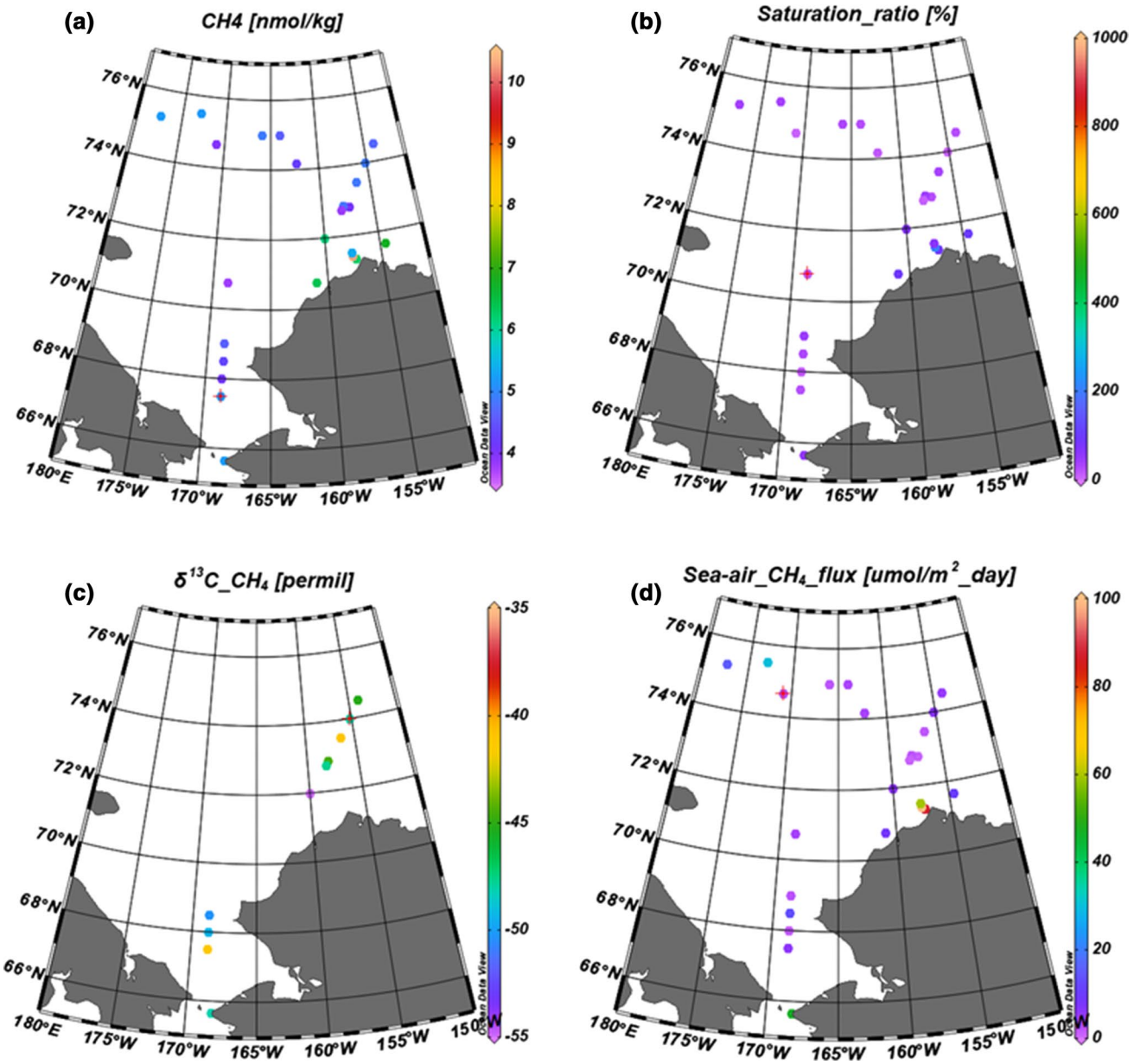

Fig. 2 Horizontal distribution of **a** concentration, **b** oversaturation ratio (SR), **c** sea–air CH_4 flux (F_{CH4}), and **d** $\delta^{13}C$ values of dissolved CH_4 in surface seawater (0–10 m depth)

3.2.2 Deeper area (from off Point Barrow to the Canada Basin)

Figure 4a–g and Table S3 present vertical distributions of CH_4, DO, physical parameters, and the N^{**} value at St. 66, 68, and 69. Defined as a linear combination of nitrate and phosphate ($N^{**} = 0.87 \times (([NO_3^-] + [NO_2^-] + [NH_4^+]) - 16\,[PO_4^{3-}] + 2.9)$ μmol kg^{-1}) was proposed to investigate the distribution of nitrogen fixation and denitrification (Gruber and Sarmiento 1997; Nishino et al. 2005). Correlations between CH_4 and phosphate and those between CH_4 and potential density are shown in Fig. 4h, i. Depth–latitude sections of CH_4 and DO from off Point Barrow to the Canada Basin are presented in Fig. 5a–d.

In general, the CH_4 concentration maximum was observed at 10–50 m depth ([CH_4], up to 17.7 nmol kg^{-1}; SR, up to 415.1%). At St. 68 and 69, there was another maximum was found at 100–200 m depth ([CH_4], up to 21.8 nmol kg^{-1}; SR, up to 477.2%). However, the $\delta^{13}C$ values showed a minimum at around 50 m depth and increased gradually below that depth (10–50 m depth, − 65.1 to − 43.5‰; 100–200 m depth, − 58.3 to − 25.7‰) at St. 66 and 69, although a secondary minimum was observed at St. 68. Dissolved CH_4 concentrations were almost all less than 5 nmol kg^{-1} and

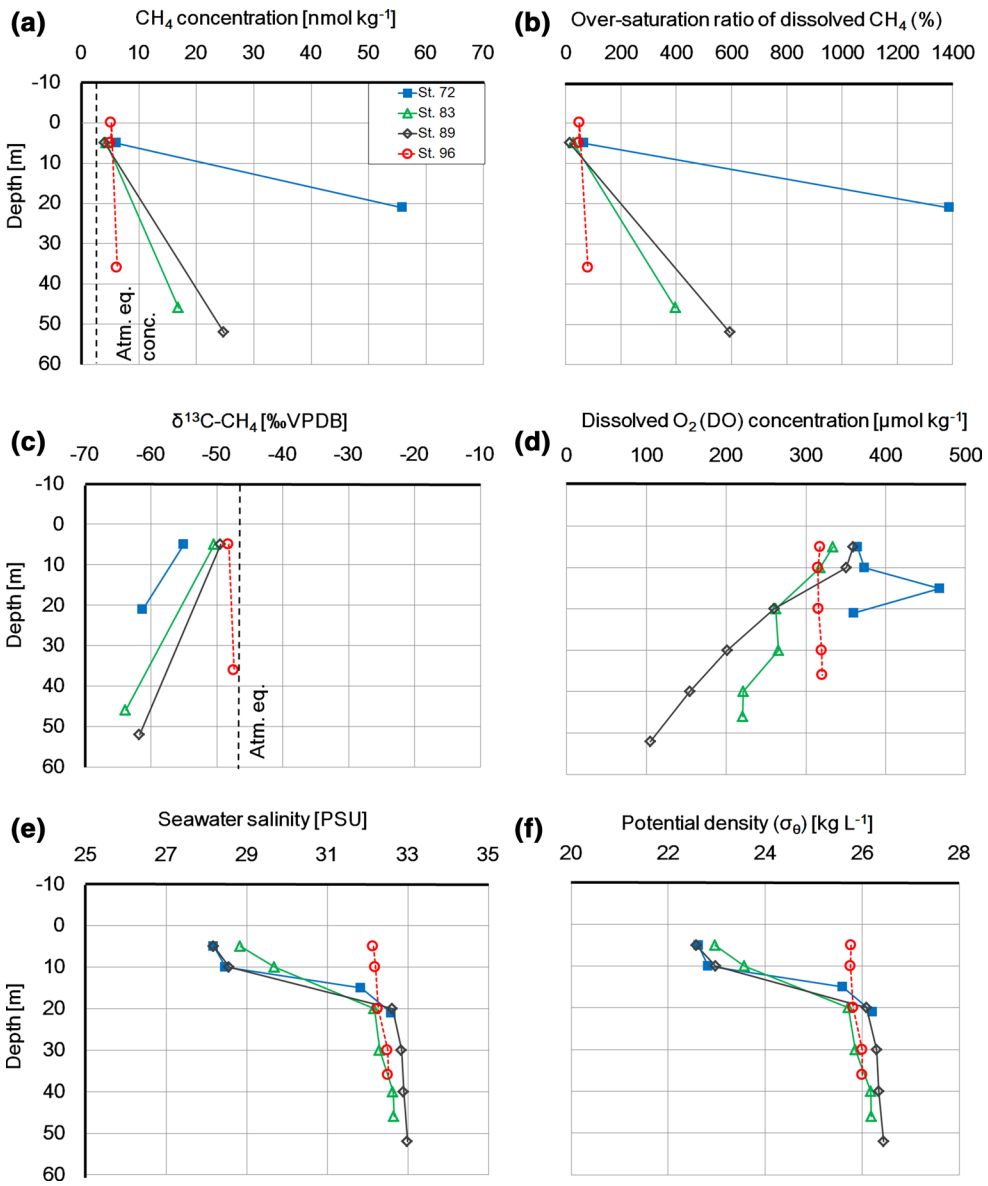

Fig. 3 Vertical distributions of **a** concentration, **b** SR, and **c** $\delta^{13}C$ values of dissolved CH_4, **d** DO concentration, **e** seawater salinity, and **f** potential density (σ_θ) in the coastal shelf area (Chukchi Sea: St. 72, 83, and 89; Bering Strait: St. 96). Data of DO concentration, seawater salinity, and potential density (σ_θ) were obtained from the JAMSTEC database

SR < 0 at several depths below 700 m depth. $\delta^{13}C$ values were close to − 40 to − 30‰ below 700 m depth.

4 Discussion

4.1 Dissolved CH_4 dynamics in surface seawater

The value of F_{CH4} calculated from the observed CH_4 concentration suggests that the western Arctic Ocean behaves as a potential CH_4 source to the atmosphere during the sea-ice free period. In addition, $\delta^{13}C_{ex}$ values of dissolved CH_4 in surface seawater indicate that biological processes produce excess CH_4.

In the continental shelf area, DO concentrations (mean, 339.5 ± 5.1 μmol kg^{-1}) were lower than in the deeper area (mean, 360.0 ± 5.1 μmol kg^{-1}) (JAMSTEC database). Furthermore, higher nutrient concentrations (up to 30.7, 2.04, 4.50, 14.1, and 0.240 μmol kg^{-1} for silicate, phosphate, ammonia, nitrate, and nitrite, respectively) produced by decomposition of organic matter deposited at the sediments (Nishino et al. 2005) were also found in this area, which suggests that excess CH_4 in the surface water is produced mainly by methanogens in seafloor sediments.

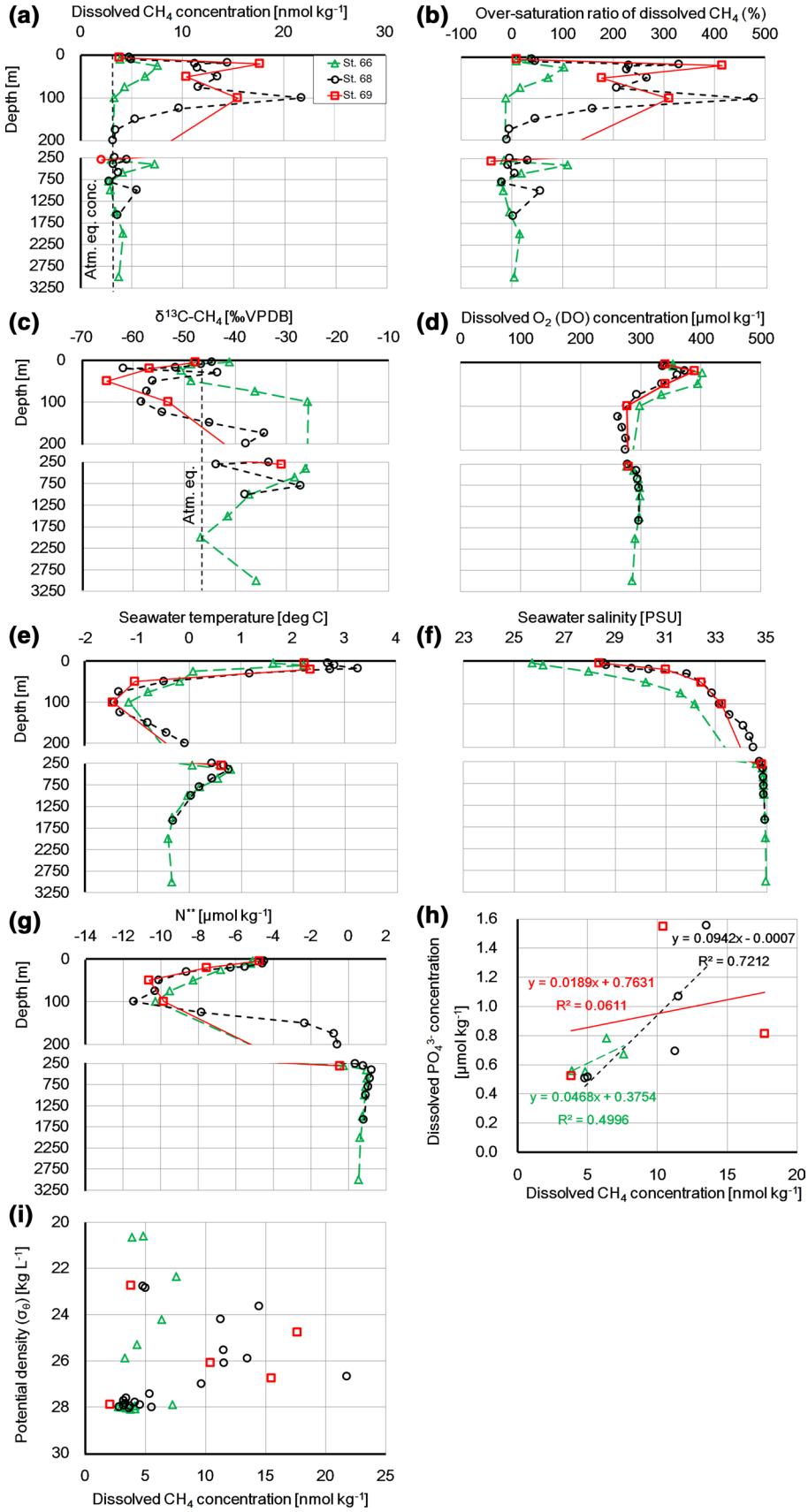

Fig. 4 Vertical distributions of **a** concentration, **b** SR, and **c** $\delta^{13}C$ values of dissolved CH_4, **d** DO concentration, **e** seawater temperature, **f** seawater salinity, and **g** N^{**} value, and correlation diagrams of **h** dissolved CH_4 concentration–dissolved phosphate (PO_4^{3-}) concentration and **i** dissolved CH_4 concentration–potential density (σ_θ) in the Canada Basin. Data of DO concentration, seawater temperature, seawater salinity, PO_4^{3-} concentration, and potential density (σ_θ) were obtained from the JAMSTEC database

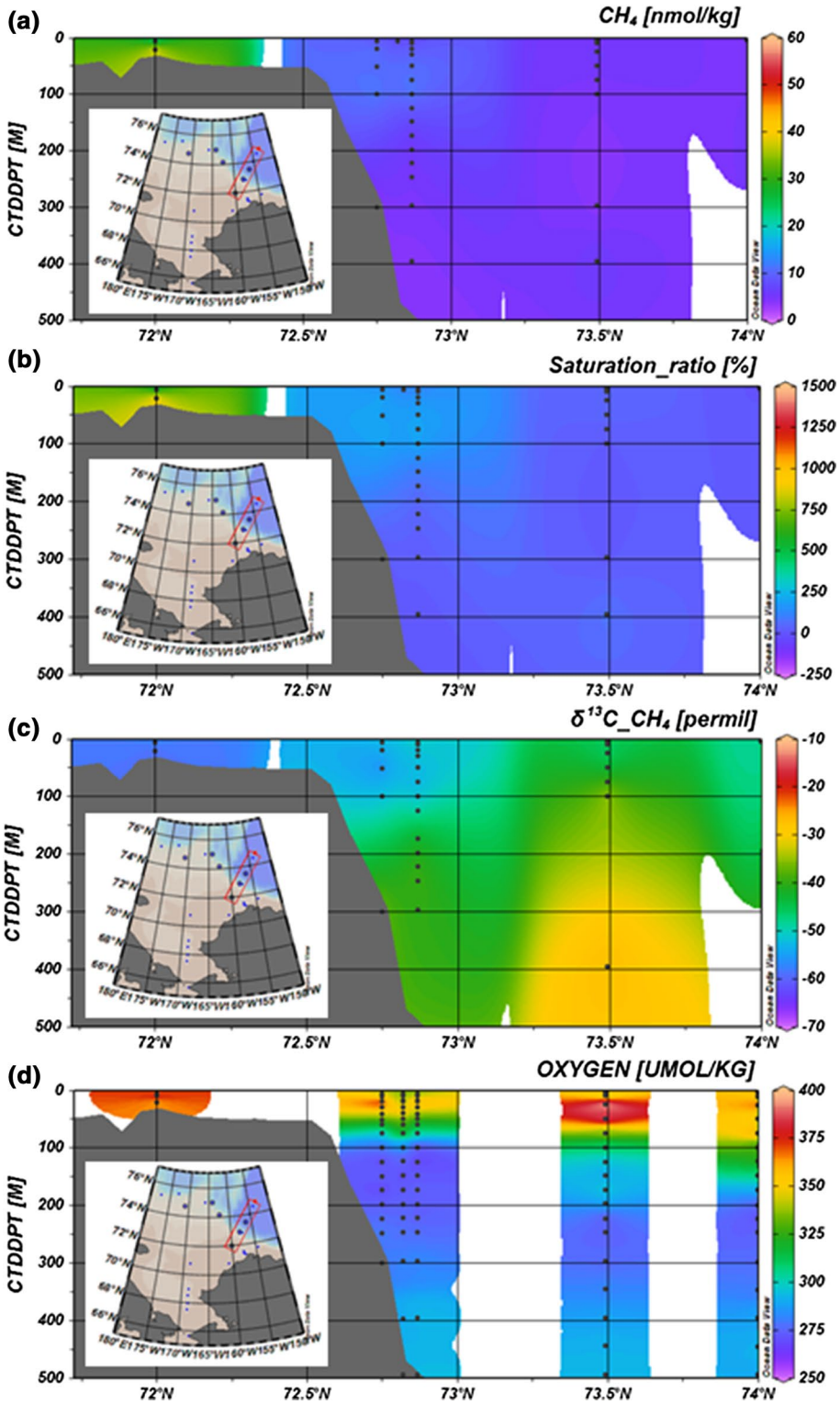

Fig. 5 Spatial distributions of **a** concentration, **b** SR, **c** $\delta^{13}C$ of dissolved CH_4, and **d** DO concentration in the deeper area. Data of DO concentration were obtained from the JAMSTEC database

In the deeper area near the Canada Basin, higher DO concentration and lower pCO_2 were observed. Higher chlorophyll-*a* (Chl. *a*) concentration (> 0.5 mg L^{-1}) was found near St. 68 and 69 (JAMSTEC database; Cruise report of MR12-E03 cruise). These tendencies indicate that photosynthesis by phytoplankton occurs well in this area, and that CH_4 might be produced mainly by phytoplankton and zoo plankton activities in this area. Therefore, dynamics of dissolved CH_4 differ between the coastal shelf area and deeper area. We discuss details related to this issue in Sect. 4.2.

4.2 Vertical distribution of dissolved CH_4

4.2.1 Continental shelf area

4.2.1.1 Chukchi Sea Concentrations of CH_4 were higher in bottom water (16.9–55.9 nmol kg^{-1}) than in surface water (4.1–6.1 nmol kg^{-1}), although concentrations of DO were lower in bottom water (104.9–359.8 µmol kg^{-1}) than in surface water (333.9–364.3 µmol kg^{-1}) in the Chukchi Sea (St. 72, 83, and 89). Similar profiles have been observed in other Arctic Ocean areas, indicating that sediments are a major CH_4 source to shelf waters (Macdonald 1976; Damm et al. 2005; Shakhova et al. 2005, 2010, 2014; Savvichev et al. 2007). Savvichev et al. (2007) reported that CH_4 concentrations in bottom layer were two times higher than in the surface layer in the Chukchi Sea. They also estimated the rates of methanogenesis from seafloor sediments in the Chukchi Sea to be as high as 67 µmol m^{-2}, i.e., dramatically higher than the rates of methane oxidation (approx. 3 µmol m^{-2}).

The $\delta^{13}C$ values in bottom water (− 63.8 to − 61.3‰) were lower than in surface water (− 55.0 to − 49.4‰). This result indicates that CH_4 is supplied from resuspension of seafloor sediments, in which particle organic matter (POM) is decomposed by methanogenic activity via CO_2 reduction pathways. In bottom water, the transmission decreased, indicating an accumulation of organic matter and its decomposition at the bottom (Nishino et al. 2016). These $\delta^{13}C$ values in bottom water were within the range of reported values of the CO_2 reduction pathway ($\delta^{13}C$ = − 110 to − 60‰: Whiticar et al. 1986, Whiticar 1999; Sugimoto and Wada 1993; Kastner et al. 1998). Furthermore, the Chukchi Sea holds Point Barrow (near St. 72) and the hollow called Hope Valley (near St. 83 and 89), where sediments are readily accumulated and where positive apparent oxygen utilization (AOU) and positive correlation between CH_4 and CO_2 (Database of JAMSTEC) are reported (Verzhbitsky et al. 2008; Yamada et al. 2015; Nishino et al. 2016).

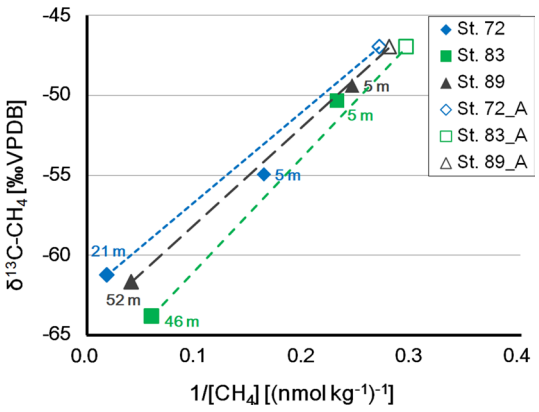

Fig. 6 Relation between inverse of dissolved CH_4 concentration (1/[CH_4]) and $\delta^{13}C$–CH_4 values at stations 72, 83, and 89. Data from two depths (5 m and bottom) are drawn as closed symbols and calculated values for the surface water equilibrated with the atmosphere (A) are drawn as open symbols. Straight lines show mixing lines between the bottom layer CH_4 and atmospheric equilibrium

A thermocline and pycnocline were found at 10–20 m depths at these stations. Myhre et al. (2016) reported that CH_4 release from seafloor sediments west of Svalbard substantially increased its concentrations in the ocean, but this release has limited influence on atmospheric CH_4 levels because of the pycnocline, except for the case in which physical processes (e.g., storms) remove this dynamic barrier (Myhre et al. 2016). When excess CH_4 in the seawater is transported, it is affected simultaneously by oxidation, dilution and mixing with atmosphere, in addition to loss into the atmosphere (Damm et al. 2005). In the Chukchi Sea, a markedly higher CH_4 production rate than CH_4 oxidation rate has been reported (Savvichev et al. 2007). Therefore, we examine the effects of mixing with atmospheric CH_4 at these stations using the relation between inverse of CH_4 concentration (1/[CH_4]) and $\delta^{13}C$ (Fig. 6). At these stations, data from 5 m depth almost fall on the mixing line between the bottom layer and atmosphere. Therefore CH_4 was produced by methanogenic activity in seafloor sediments and was partially transported strongly to the surface, affected mainly by mixing between atmospheric CH_4. Fenwick et al. (2017) observed dissolved CH_4 in the Bering Sea and Chukchi Sea in July–October 2015. They concluded that this CH_4 was produced from methanogens in seafloor sediments from the decomposition of organic carbon. Then microbial CH_4 oxidation occurred, as inferred from information related to the concentration (0.7–30.5 nmol L^{-1}) and $\delta^{13}C$ (from − 42 to − 33‰) of CH_4. The vertical gradients of CH_4 concentrations and the CH_4 concentrations in bottom water (approx. 10–31 nmol L^{-1}) reported by Fenwick et al. (2017) were respectively weaker and lower than our data. Furthermore, they observed higher $\delta^{13}C$ values than those found in the present study. These differences might derive from CH_4 release from seafloor sediments and the strength of stratification by sea-ice melt water. Lapham et al. (2017) reported using data from August 2012 when most of the water column CH_4 profiles in Barrow Canyon exhibited an increase with

depth (5–74 nmol L^{-1}), suggesting that mainly sedimentary sources produced CH_4. The $\delta^{13}C$ profiles obtained in the same area during this study agree with such sedimentary CH_4 production.

4.2.1.2 Bering Strait In the Bering strait in October (St. 96), the concentration and $\delta^{13}C$ values of CH_4 in seawater become almost homogeneous from the surface water to bottom water, showing values close to those expected under equilibrium with the atmosphere. Furthermore, DO concentration and potential density also become homogeneous from the surface water to bottom water (Fig. 3d, e; Database of JAMSTEC). These tendencies suggest that CH_4 is well mixed between bottom water and surface water because of surface water cooling in mid-October, in addition to a small influence by sea-ice melt water. Only a single profile was obtained in this region. Nevertheless, these facts might suggest weaker CH_4 emissions in the Bering Strait than in the Chukchi Sea.

4.2.2 Deeper area

Two CH_4 concentration maxima were observed at 10–50 m depth and 100–200 m depth, whereas the DO concentration maximum was observed only at around 10–50 m depth. Nutrient concentration maxima were observed only at around 100–200 m depth. In the following sections, we discuss CH_4 production processes in the shallower (10–50 m) and deeper (100–200 m) CH_4 maxima.

4.2.2.1 Shallower CH_4 maximum At 10–50 m depth, the CH_4 concentration increased and $\delta^{13}C$ decreased concomitantly with depth. Positive correlation was found between CH_4 and phosphate concentrations (Fig. 4h). Apparent correlation between dissolved CH_4 and phosphate concentrations has been also observed in Pdw in the central Arctic Ocean ($y = 0.1161x - 0.1473$, $R^2 = 0.8823$) (Damm et al. 2010). Damm et al. (2010) also found negative correlation between dissolved CH_4 and DMSP, a metabolite of phytoplankton in the Pdw. They proposed that CH_4 was produced by bacteria from DMSP in nitrate-depleted and phosphate-rich aerobic water. During our observations in the western Arctic Ocean, nitrate deficits and phosphate concentration were greater (N^* values and phosphate concentrations were, respectively, − 11.9 to − 4.5 µmol kg^{-1} and 0.5–1.6 µmol kg^{-1}) than in the Pdw reported by Damm et al. (2010) ($N^* = -1.5$ to + 1 µmol kg^{-1} and $[PO_4^{3-}] = 0.4$–0.9 µmol kg^{-1}, respectively). Therefore, it is likely that at least a part of the excess CH_4 was produced from DMSP, although we have no data for DMSP. However, accumulation of particle organic car-

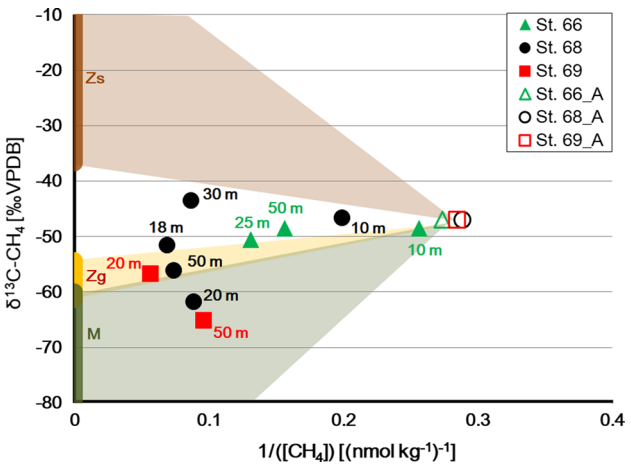

Fig. 7 Relation between inverse of dissolved CH_4 concentration (1/[CH_4]) and $\delta^{13}C$–CH_4 values in 10–50 m depth at stations 66, 68, and 69. Data from 10–50 m depth are drawn as closed symbols and calculated values for the surface water equilibrated with the atmosphere (A) are drawn as open symbols. Three zones show mixing between each of three end-members: Zs, sinking particle from zooplankton body ($\delta^{13}C_{Zs}$ = from − 37 to + 6‰; Sasakawa et al. 2008); Zg, zooplankton guts ($\delta^{13}C_{Zg}$ = from − 61 to − 54‰; Sasakawa et al. 2008); M, methanogen (CO_2 reduction pathway) [$\delta^{13}C_M$ = from − 110 to − 60‰; Whiticar et al. 1986; Whiticar 1999; Sugimoto and Wada 1993)] and the surface water

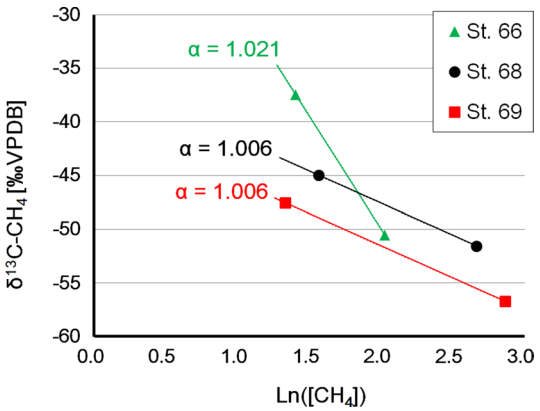

Fig. 8 Oxidation line between CH_4 concentration maximum in 10–50 m depth and 0–10 m depth

Table 1 Distribution of dissolved CH_4 concentrations, $\delta^{13}C$ values, and α values at St. 66, 68, 69 (at 100 m depth), and 72 (at 21 m depth)

Station	Depth (m)	[CH_4] (nmol kg^{-1})	$\delta^{13}C$ (‰ VPDB)	α
66	100	3.3	− 25.7	1.018
68	100	21.8	− 58.3	–[a]
69	100	15.5	− 53.1	1.006
72	21	55.9	− 61.3	–[a]

[a]Values in these points cannot be calculated because of increasing CH_4 concentrations

bon (POC) and Chl. *a* was observed near St. 68 immediately above the pycnocline (0–60 m depth; Yamada et al. 2015). This fact suggests that CH_4 is also produced by methanogenic activity in zooplankton guts or sinking particles from zooplankton. Figure 7 shows mixing between atmospheric equilibrium and three end-members: (1) sinking particles from zooplankton (Zs) and (2) zooplankton guts (Zg). Methane from these end-members was produced originally by (3) methanogens via the CO_2 reduction pathway (C_M). The CH_4 is partly consumed by microbial CH_4 oxidation with ^{13}C enrichment of remaining CH_4 within these anaerobic microenvironments (Oremland 1979; Karl and Tilblook 1994; Holmes et al. 2000; Sasakawa et al. 2008). Figure 7 suggests that CH_4 is produced by methanogenic activity within zooplankton guts or sinking particles in addition to DMSP at 10–50 m depth in summer in the Canada Basin. However, the largest $\delta^{13}C$ values (–43‰) are still lower than those of sinking particles, which indicates that CH_4 was produced mainly from zooplankton guts and methanogens, and that it was not well oxidized within sinking particles. Furthermore, if one assumes a decrease in CH_4 concentrations from CH_4 maxima (10–50 m depth) to 0–10 m depth results from CH_4 oxidation, then the α values are calculated as $\alpha = 1.021$, 1.006, and 1.006 at St. 66, 68, and 69, respectively (Fig. 8). Those calculated values agree with values of biological aerobic–anaerobic CH_4 oxidation reported from earlier studies (1.005–1.035; Coleman et al. 1981; Alperin et al. 1988; Martens et al. 1999; Tsunogai et al. 2000; Sansone et al. 2001). This fact indicates that CH_4 produced by zooplankton/phytoplankton activity might be transported vertically from 10–50 m depth to 0–10 m depth: then it is oxidized by biological oxidation.

4.2.2.2 Deeper CH_4 maximum At 100–200 m depth, the concentration and $\delta^{13}C$ values of dissolved CH_4 in seawater became lower and higher as dissolved CH_4 gas left the bottom of the continental shelf area off Point Barrow (St. 72), except at around St. 68 (Fig. 5a–c, Table 1). This dissolved CH_4 might be transported laterally along the extended shelf water and Alaskan Continental Current (Hioki et al. 2014; Gong and Pickart 2015; Zhang et al. 2015). Hioki et al. (2014) measured dissolved Fe, humic-like fluorescent, dissolved organic matter, and nutrient concentrations in waters above the continental shelf area (Chukchi Sea) and deeper area (Canada Basin) during the same cruise as this study. They inferred lateral transportation of these constituents from shelf sediments to basin regions (Hioki et al. 2014). Results of several earlier studies suggest that particles in the shelf region are transferred to the slope–basin region by water currents from the Bering Strait to the Canada Basin (Aagaard et al. 2006; Hopcroft et al. 2008; Yamada et al. 2015). Here, we suggest that dissolved CH_4 was also transported horizontally from the continental shelf to the Canada Basin (in 100–200 m depth).

Furthermore, α values ($\alpha = 1.006$ and 1.018, respectively, at St. 72–69 and St. 68–66 (Table 1)), indicate that CH_4 was affected not only by dilution but also by CH_4 consumption from biological oxidation. If biogenic CH_4 production occurred, then the isotopic enrichment around the CH_4 concentration maximum zone indicated that the CH_4 was produced elsewhere and that it subsequently underwent partial bacterial oxidation and isotopic fractionation (Coleman et al. 1981; Sansone et al. 2001). Sansone et al. (2001) suggested that the isotopically heavy CH_4 was not from local production by methanogens, but was instead attributable to biological oxidation with CH_4 advection from CH_4 maxima occurring along the eastern margin of the Pacific. Furthermore, Yoshikawa et al. (2014) showed that the ^{13}C-enriched CH_4 (> -30‰) originated not only from in situ CH_4 production and oxidation but also from the CH_4 transported from the eastern upwelling region off Peru. However, when data from St. 68 and 69 obtained at the 100–200-m-depth area were compared, the CH_4 concentration was found to be higher at St. 68 than at St. 69. A lower $\delta^{13}C$ value was found at St. 68 than at St. 69 (Table 1), which indicates that in situ CH_4 production might occur by methanogen in particles. Therefore, after CH_4 was produced mainly by methanogens in continental shelf sediments, it was transported horizontally to the Canada Basin (100–200 m depth) with effects not only by biological oxidation but also by methanogens in particles.

5 Conclusions

We analyzed concentrations and $\delta^{13}C$ values of dissolved CH_4 in the western Arctic Ocean during the R/V Mirai cruise of 3 September–17 October, 2012 (MR12-E03 cruise), when the sea-ice extent was minimal. Surface water was found to be supersaturated with CH_4 in all cases, suggesting that the western Arctic Ocean behaved as a potential CH_4 source to the atmosphere during summer. In the Chukchi Sea, higher CH_4 concentrations in the bottom layer were produced mainly by methanogens in continental shelf sediments, as indicated by their accompanying $\delta^{13}C$ values (< -60‰); CH_4 in the surface layer was mixed between the bottom layer and atmosphere. In the Canada Basin, maxima of CH_4 concentration were detected at 10–50 and 100–200 m depths. Profiles of $\delta^{13}C$ and DO concentration indicate that shallower CH_4 maxima were produced by guts in zooplankton, sinking particles, and phytoplankton metabolite (e.g., DMSP), whereas deeper CH_4 maxima were produced by methanogen in continental shelf sediments, with transportation horizontally to the Canada Basin with effects from both CH_4 production by particle and biological CH_4 oxidation. Results obtained from this study clarified the horizontal

and vertical profiles of dissolved CH_4 in the western Arctic Ocean. These results are expected to contribute to our understanding of the feedback effects to Arctic climate change.

Acknowledgements We acknowledge the scientists and crews of the MR12-E03 cruise on R/V Mirai, JAMSTEC, for sampling and providing the hydrographic and nutrient data. This study was conducted under the Green Network of Excellence (GRENE) Arctic Climate Change Research Project. It was also supported financially by JSPS KAKENHI 23224013 and by the Global COE program "From Earth to Earths" of the Ministry of Education, Culture, Sports, Science and Technology, Japan. Figures 1, 2, and 5 were drawn using "Ocean Data View" (http://odv.awi.de/) software. The data used to prepare Figs. 3, 4 and 5 are available from the Data Research System for Whole Cruise Information in JAMSTEC (Darwin; http://www.godac.jamstec.go.jp/darwin/cruise/mirai/mr12-e03/e).

References

Aagaard K, Weingartner TJ, Danielson SL, Woogate RA, Johnson GC, Whitledge TE (2006) Some controls on flow and salinity in Bering Strait. Geophys Res Lett 33:L19602. https://doi.org/10.1029/2006GL026612

Alperin MJ, Reeburgh WS, Whiticar MJ (1988) Carbon and hydrogen isotope fractionation resulting from anaerobic methane oxidation. Glob Biochem Cycles 2:279–288

Arrigo KR, van Dijken G (2011) Secular trends in Arctic Ocean net primary production. J Geophys Res 116:C09011. https://doi.org/10.1029/2011JC007151

Coleman DD, Risatti JB, Schoell M (1981) Fractionation of carbon and hydrogen isotopes by methane-oxidizing bacteria. Geochim Cosmochim Acta 45:1033–1037

Damm E, Mackensen A, Budeus G, Faber E, Hanland C (2005) Pathways of methane in seawater: plume spreading in an Arctic shelf environment (SW-Spitsbergen). Cont Shelf Res 25:1453–1472

Damm E, Kiene RP, Schwarz J, Flack E, Dieckmann G (2008) Methane cycling in Arctic shelf water and its relationship with phytoplankton biomass and DMSP. Mar Chem 109:45–59

Damm E, Helmke E, Thoms S, Schauer U, Nothig E, Bakker K, Kiene RP (2010) Methane production in aerobic oligotrophic surface water in the central Arctic Ocean. Biogeoscience 7:1099–1108

Damm E, Rudels B, Schauer U, Dieckmann G (2015) Methane excess in Arctic surface water-triggered by sea ice formation and melting. Sci Rep 5:16179

Dlugokencky EJ, Bruhwiler L, White JWC, Emmons LK, Novelli PC, Montzka SA, Masarie KA, Lang PM, Crotwell AM, Miller JB, Gatti LV (2009) Observational constraints on recent increases in the atmospheric CH_4 burden. Geophys Res Lett 36:L18803. https://doi.org/10.1029/2009GL039780

Dlugokencky EJ, Nisbet EG, Fisher RE, Lowry D (2011) Global atmospheric methane: budget, changes and dangers. Philos Trans R Soc A 369:2058–2072

Fenwick L, Capelle D, Damm E, Zimmermann S, Williams WJ, Vagle S, Tortell PD (2017) Methane and nitrous oxide distributions across the North American Arctic Ocean during summer, 2015. J Geophys Res Oceans 122:390–412. https://doi.org/10.1002/2016JC012493

Gong D, Pickart RS (2015) Summertime circulation in the eastern Chukchi Sea. Deep Sea Res Part 2(118):18–31

Grant NJ, Whiticar MJ (2002) Stable carbon isotopic evidence for methane oxidation in plumes above Hydrate Ridge, Cascadia Oregon Margin. Glob Biogeochem Cycles 16:4. https://doi.org/10.1029/2001GB001851

Gruber N, Sarmiento JL (1997) Global patterns of marine nitrogen fixation and denitrification. Glob Biogeochem Cycles 11(2):235–266

Harada N (2016) Review: potential catastrophic reduction of sea ice in the western Arctic Ocean: Its impact on biogeochemical cycles and marine ecosystems. Glob Planet Change 136:1–17

Hioki N, Kuma K, Morita Y, Sasayama R, Ooki A, Kondo Y, Obata H, Nishioka J, Yamashita S, Kikuchi T, Aoyama M (2014) Laterally spreading iron, humic-like dissolved organic matter and nutrients in cold, dense subsurface water of the Arctic Ocean. Sci Rep 4:6775. https://doi.org/10.1038/srep06775

Holmes ME, Sansone FJ, Rust TM, Popp BN (2000) Methane production, consumption, and air–sea exchange in the open ocean: an evaluation based on carbon isotopic ratios. Glob Biogeochem Cycles 14(1):1–10

Hopcroft R, Bluhm B, Gradinger R (2008) Arctic Ocean synthesis: analysis of climate change impacts in the Chukchi and Beaufort Seas with strategies for future research. University of Alaska Fairbanks, Institute of Mar. Sci., 184 pp., North Pacific Research Board, Anchorage, Alaska

Intergovernmental Panel on Climate Change AR4 (2007)

Intergovernmental Panel on Climate Change AR5 (2013)

Karl DM, Tilblook BD (1994) Production and transport of methane in oceanic particulate organic matter. Nature 368:732–734

Kastner M, Kvenvolden KA, Lorenson TD (1998) Chemistry, isotopic composition, and origin of a methane–hydrogen sulfide hydrate at the Cascadia subduction zone. Earth Planet Sci Lett 156:173–183

Kikuchi T (2012) R/V Mirai Cruise Report MR12-E03. In: Kikuchi T, Nishino S (eds) JAMSTEC, Yokosuka, Japan, p 190

Kvenvolden KA (1993) Gas hydrates—geological perspective and global change. Rev Geophys 31(2):173–187

Kvenvolden KA, Lilley MD, Lorenson TD, Barnes PW, McLaughlin E (1993) The Beaufort Sea continental shelf as a seasonal source of atmospheric methane. Geophys Res Lett 20(22):2459–2462

Lapham L, Marshall K, Magen C, Lyubchich V, Cooper LW, Grebmeier JM (2017) Dissolved methane concentration in the water column and surface sediments of Hanna Shoal and Barrow Canyon, northern Chukchi Sea. Deep Sea Res II 144:92–103. https://doi.org/10.1016/j.dsr2.2017.01.004

Macdonald RW (1976) Distribution of low-molecular weight hydrocarbons in southern Beaufort Sea. Environ Sci Technol 10:1241–1246

Martens CS, Albert DB, Alperin MJ (1999) Stable isotope tracing of anaerobic methane oxidation in the gassy sediments of Eckernfoerde Bay, German Baltic Sea. Am J Sci 299:589–610

McGuire AD, Anderson LG, Christensen TR, Dallimore S, Guo L, Hayes DJ, Heimann M, Lorenson TD, Macdonald RW, Roulet N (2009) Sensitivity of the carbon cycle in the Arctic to climate change. Ecol Monogr 79(4):523–555

McGuire AD, Macdonald RW, Schuur EAG, Harden JW, Kuhry P, Hayes DJ, Christensen TR, Heimann M (2010) The carbon budget of the northern cryosphere region. Curr Opin Environ Sustain 2:231–236

Myhre CL, Ferre B et al (2016) Extensive release of methane from Arctic seabed west of Svalvard during summer 2014 does not influence the atmosphere. Geophys Res Lett 43:4624–4631. https://doi.org/10.1002/2016GL068399

Nishino S, Shimada K, Itoh M (2005) Use of ammonium and other nitrogen tracers to investigate the spreading of shelf waters in the western Arctic Ocean. J Geophys Res 110:C10005. https://doi.org/10.1029/2003-JC002118

Nishino S, Kikuchi T, Fujiwara A, Hirawake T, Aoyama M (2016) Water mass characteristics and their temporal changes in a biological hotspot in the southern Chukchi Sea. Biogeosciences 13:2563–2578. https://doi.org/10.5194/bg-12-2563-2016

Oremland RS (1979) Methanogenic activity in plankton samples and fish intestines: a mechanism for in situ methanogenesis in oceanic surface waters. Limnol Oceanogr 24(6):1136–1141

Permenteir F-JW, Christensen TR, Sorensen LL, Rysgaard S, McGuire AD, Miller PA, Walker DA (2013) The impact of lower sea-ice extent on Arctic greenhouse-gas exchange. Nat Clim Change 3:195–202. https://doi.org/10.1038/nclimate1784

Quay PD, King SL, Stutsman J, Wilbur DO, Steele LP, Fung I, Gammon RH, Brown TA, Farwell GW, Grootes PM, Schmidt FH (1991) Carbon isotopic composition of atmospheric methane: fossil and biomass burning source strength. Glob Biogeochem Cycles 5:25–47

Sansone FJ, Popp BN, Gase A, Graham AW, Rust TM (2001) Highly elevated methane in the eastern tropical north Pacific and associated isotopically enriched fluxes to the atmosphere. Geophys Res Lett 24:4567–4570

Sasakawa M, Tsunogai U, Kameyama S, Nakagawa F, Nojiri Y, Tsuda A (2008) Carbon isotopic characterization for the origin of excess methane in subsurface seawater. J Geophys Res 113:C03012. https://doi.org/10.1029/2007JC004217

Savvichev AS, Rusanov II, Pimenov NV, Zakharova EE, Veslopolpva EF, Lein AL, Crane K, Ivanov MV (2007) Microbial processes of the carbon and sulfur cycles in the Chukchi Sea. Mikrobiologiia 76(5):682–693. https://doi.org/10.1134/S00262617070S0141

Shakhova N, Semiletov I, Panteleev G (2005) The distribution of methane on the Siberian Arctic shelves: implications for the marine methane cycle. Geophys Res Lett 32:L09601. https://doi.org/10.1029/2005GL022751

Shakhova N, Semiletov I, Salyuk A, Yusupov V, Kosmach D, Gustafsson O (2010) Extensive methane venting to the atmospheric from sediments of the east Siberian Arctic shelf. Science 327:1246. https://doi.org/10.1126/science.118221

Shakhova N, Semiletov I, Leifer I, Sergienko V, Salyuk A, Kosmach D, Stubbs C, Nicolsky D, Tumskoy V, Gustafsson O (2014) Ebullition and storm-induced methane release from the East Siberian Arctic Shelf. Nat Geosci 7:64–70. https://doi.org/10.1038/ngeo2007.

Sugimoto A, Wada E (1993) Carbon isotopic composition of bacterial methane in a soil incubation experiment: contributions of acetate and CO_2/H_2. Geochim Cosmochim Acta 57:4015–4027

Tsunogai U, Ishibashi J, Wakita H, Gamo T, Watanabe K, Kajimura T, Kanayama S, Sakai H (1998) Methane rich plumes in Suruga Trough (Japan) and their carbon isotopic characterization. Earth Planet Sci Lett 160:97–105

Tsunogai U, Yoshida N, Ishibashi J, Gamo T (2000) Carbon isotopic distribution of methane in deep-sea hydrothermal plume, Myojin Knoll Caldera, Izu-Bonin arc: implications for microbial methane oxidation in the oceans and applications to heat flux estimation. Geochim Cosmochim Acta 64(14):2439–2452

Verzhbitsky V, Savostina T, Frantzen E, Little A, Sokolov SD, Tuchkova MI (2008) The Russian Chukchi Sea shelf. GEO ExPro 5(3):36–41

Wanninkhof R (1992) Relationship between wind speed and gas exchange over the ocean. J Geophys Res 97(C5):7373–7382

Watanabe S, Higashitani N, Tsurushima N, Tsunogai S (1995) Methane in the western North Pacific. J Oceanogr 51:39–60

Whiticar MJ (1999) Carbon and hydrogen isotope systematics of bacterial formation and oxidation of methane. Chem Geol 161:291–314

Whiticar MJ, Faber E, Schoell M (1986) Biogenic methane formation in marine and freshwater environments: CO_2 reduction vs. acetate fermentation—isotope evidence. Geochim Cosmochim Acta 50:693–709

Wiesenberg DA, Guinasso NL Jr (1979) Equilibrium solubilities of methane, carbon monoxide, and hydrogen in water and sea water. J Chem Eng Data 24(4):356–360

Yamada K, Yoshida N, Nakagawa F, Inoue G (2005) Source evaluation of atmospheric methane over western Siberia using double stable isotopic signatures. Org Geochem 36:717–726

Yamada Y, Fukuda H, Uchimiya M, Motegi C, Nishino S, Kikuchi T, Nagata T (2015) Localized accumulation and a shelf-basin gradient of particles in the Chukchi Sea and Canada Basin, western Arctic. J Geophys Res Oceans 120:4638–4653. https://doi.org/10.1002/2015JC010794

Yoshikawa C, Hayashi E, Yamada K, Yoshida O, Toyoda S, Naohiro Y (2014) Mathane sources and sinks in the subtropical South Pacific along 17°S as traced by stable isotope ratios. Chem Geol 382:24–31

Zhang J, Zhan L, Chen L, Li Y, Chen J (2015) Coexistence of nitrous oxide undersaturation and oversaturation in the surface and subsurface of the western Arctic Ocean. J Geophys Res Oceans 120:8392–8401. https://doi.org/10.1002/2015JC011245